The Dynamic Load Model for Medium Voltage Cascaded H-Bridge Multi-Level Inverter fed IM Drive System using Fuzzy Logic Controller

V. Raja Sekhar[*1]**, S. Sridhar**[2]** , B. Sree Bhavani**[3]

[*1]PG Scholar in Electrical Department, JNT University, Anantapur, Andhra Pradesh, India
[2]Asstistant Professor Electrical Department, JNT University, Anantapur, Andhra Pradesh, India
[3]M. Tech Electrical Department, Sreenidhi institute of Science Technology, Anantapur, Andhra Pradesh, India

ABSTRACT

This paper proposes a detailed switching model for the medium voltage cascaded H-bridge multi level inverter drive and induction motor system using fuzzy logic controller which is suitable for power system dynamic studies. The model includes the aggregated effect of an MVD, an induction motor, and their control system, and thus, it can accurately represent the dynamic responses of the motor drive system under Disturbances. Voltage and frequency both are depended on system modelling. The efficiency of the model is varied by a case study. A sensitivity study is conducted to evaluate the impact of the model parameter variation on dynamic response characteristics. The developed detailed switching model using fuzzy logic controller can be readily inserted in the large-scale power system simulation software for power system dynamic studies.
Keywords: Cascaded H-Bridge Multi-Level Inverter, Frequency Dependence, Load Model, Medium Voltage Drives (MVDs), Power System Dynamic Studies, Voltage Dependence.

I. INTRODUCTION

IT HAS been perceived for over two decades that portrayals of energy system loads for dynamic performance examination can have significant affect on control system soundness. As power systems are planned and worked with a lower soundness edge, sufficient load models are of major significance [1], [2]. Regardless of colossal research endeavours and gained learning, stack demonstrating stays a standout amongst the most questionable ranges in huge scale control system reproductions due to the changing idea of burdens and the development of new sorts of burdens, for example, factor recurrence drives (VFDs).

VFDs are generally utilized as a part of different mechanical divisions. The displaying requirements for such gadgets turn out to be more important as their entrance level in control systems increments after some time. Power electronic gadgets including VFDs were widely examined for displaying before. Such examinations were generally cantered around the arrived at the midpoint of modelling technique for converters/rectifiers at the part level [3][11]. The

dynamic averaged-value model (AVM) of a low-voltage three-phase stack commutated converter is proposed in [11] utilizing differential conditions. In any case, the display is just at the converter level, whatever is left of the parts. outing the DC bridge, the inverter, the acceptance motor associated with the inverter yield, and the related control system for the general motor drive system are definitely not demonstrated [11].

In spite of the fact that a detailed switching mode for a VFD, an motor furthermore, their control system can be manufactured utilizing Matlab/Simulink, it can't be embedded in expansive scale control system re-enactment programming for control system dynamic examinations [5][10].

or, on the other hand the conditions in addition to specie values for the parameters (e.g., coefficients, examples) of the conditions. There are two sorts of load models: static and dynamic load models. The static load demonstrates includes logarithmic conditions. It is essentially utilized for static load parts, for example, resistive and lighting loads. The dynamic load show includes distinction or, on the other hand differential conditions [1].

Two sorts of dynamic load models are proposed for extensive modern loads in [12]: an exchange work display and a composite load demonstrate (an acceptance motor in parallel with a shunt static load). The dynamic load display communicated by an exchange work for control matrix is prescribed in [13] and [14], which gives off an impression of being a very much acknowledged dynamic stack show organize.

Medium voltage drives (MVDs) are regularly utilized as a part of high power applications and show significant impacts on the general system flow because of their substantial size and high control request. Creating sufficient dynamic load models for medium voltage motor drive systems is fundamental for control system dependability ponders.

In this paper, a detailed switching model of a medium voltage cascaded H-bridge multi-level inverter drive and an acceptance motor system is introduced. The proposed show is communicated by exchange works and can be promptly utilized as a part of substantial scale control system recreation programming, for example, PSS/E.

## II. DEVELOPMENT OF DYNAMIC LOAD MODEL

The medium voltage cascaded H-bridge multi-level inverter drives are one of the topologies for high power applications. The drive is built utilizing a series of low voltage control modules. Typically, 9 control modules shape a 18-pulse system, and 12 control modules shape a 24-pulse system at the drive input. The topology of a 9-control module 18-pulse medium voltage drive can be found. For these 18-pulse drives, there are three power modules in a phase leg, and the drives can create as much as 1,440 V line-to-neutral, or, then again 2,494 V line-to-line at the yield. The topology of a nine-control module 18-pulse medium voltage drive and an enlistment motor system is appeared in Figure 1(a).

Correspondingly, for 24-pulse drives with four power modules in a phase leg, the drives can deliver line-to-impartial voltage up to 1,920 V (line-to-arrange voltage to 3,325 V). At the drive contribution, there is a phase moving transformer At the drive input, there is a phase-shifting transformer. The phase-shift angle differs by

multiples of 20_ for 18-pulse drives and by multiples of 15_ for 24-pulse drives.

Each power module is a static pulse-width-modulated (PWM) control converter. It comprises of a three-phase full extension diode converter, a DC bridge, and a solitary phase full extension inverter. The schematic chart of each control module is appeared in Figure 1(b).

The three-phase full bridge diode converter is precisely the same as the low voltage 6-pulse drive, which is fit for accepting information control from one of the phase moving transformer optional windings at 480 V, 50/60 Hz, and charging a DC bridge capacitor to about 600 V dc voltage. The DC voltage nourishes a solitary phase full bridge inverter, which is conveyed to a solitary phase stack at any voltage up to 480 V. The yields of numerous single- phase inverters are associated in arrangement, sustaining one period of an acceptance motor. The yields of the single-phase full bridge inverters associated with phase an of an acceptance motor are shown in Figure 1(c).
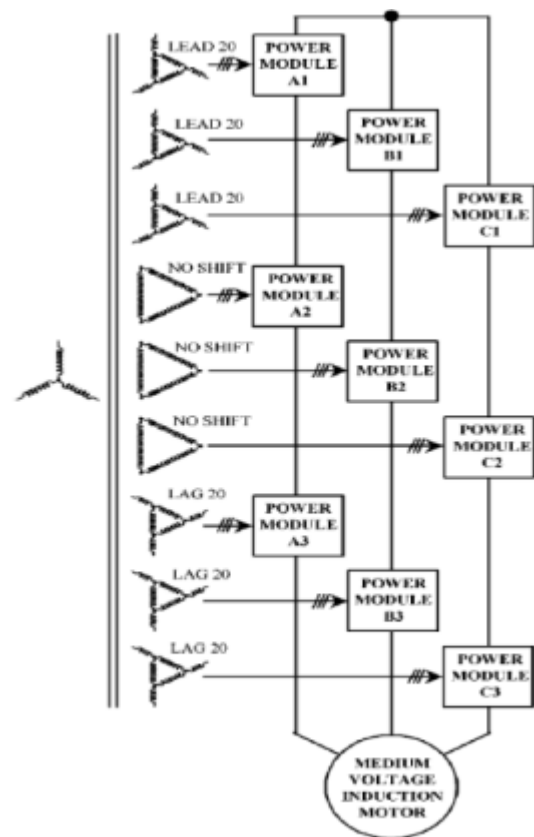
(a)
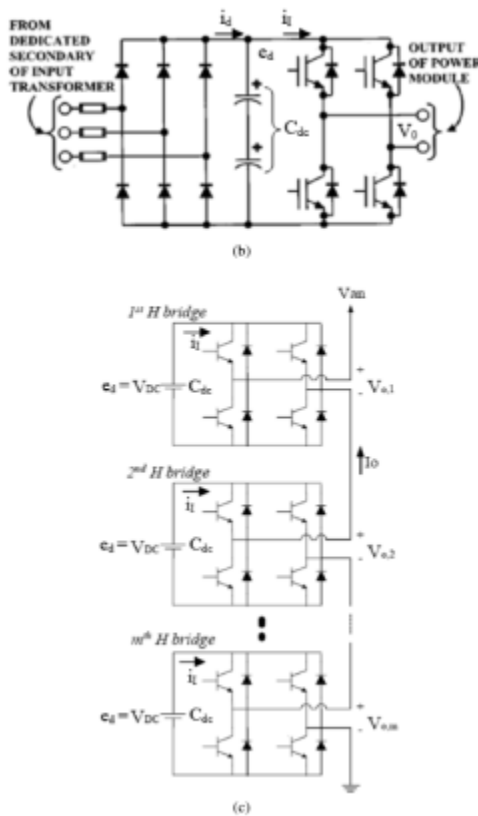
Figure 1. Eighteen-pulse cascaded H-bridge multi-level inverter motor drive system: (a) the topology of a nine-power-module drive ; (b) the schematic diagram for each power module; (c) outputs of the single-phase full bridge inverters bridged to phase a of an induction motor

A. Modelling Of The Inverter For Each Power Module

It is verified in this examination that the DC bridge voltage from the diode converter associated with the transformer secondary twisting with a phase moving edge not equivalent to are precisely the same as that from the diode converter associated with the transformer optional twisting with a phase moving edge equivalent to 0°. In this way, the phase move edge of the transformer winding does not influence the DC interface voltage from the converter in each power module. The yield voltage from the single-phase full scaffold inverter for each power module can be resolved as takes after:

$$V_0 = de_d \qquad (1)$$

where V0 is the output voltage from each power module is duty cycle, ed is the DC link voltage before the inverter.

The line to neutral voltage of the induction motor at phase aVan can be determined as follows:

$$V_{an} = \left(\frac{n_{pulse}}{6}\right) de_d \cos(\omega_s t) \qquad (2)$$

where, n pulse is the pulse number of the medium voltage drive, !s is the stator electrical field angular velocity in rad/s for the induction motor.

For an 18-pulse medium voltage drive, three power modules per phase are bridgeed to the induction motor. The pulse
number npulse is assigned as follows:

$$n_{pulse} = 18. \qquad (3)$$

The voltages at phases b and c can be determined similarly as phase a by the following equations

$$V_{bn} = \left(\frac{n_{pulse}}{6}\right) de_d \cos\left(\omega_s t - \frac{2\pi}{3}\right) \qquad (4)$$

$$V_{cn} = \left(\frac{n_{pulse}}{6}\right) de_d \cos\left(\omega_s t + \frac{2\pi}{3}\right). \qquad (5)$$

The three phase line-to-neutral voltages of the induction motor in the abc frame are converted to the dq0 frame by

$$V_{qs} = \left(\frac{n_{pulse}}{6}\right) de_d \qquad (6)$$

$$V_{ds} = 0 \qquad (7)$$

where vqs is the q-axis voltage at the terminal of the induction motor, and vds is the d-axis voltage at the terminal of the induction motor.

The real power supplied to the induction motor Pac_IM can be expressed as follows:

$$P_{ac\_IM} = \frac{3}{2}\left(V_{ds}i_{qs} + V_{qs}i_{qs}\right) = \frac{3}{2}V_{qs}i_{qs}$$

$$= \frac{3}{2} \times \left(\frac{n_{pulse}}{6} de_d\right) i_{qs} = \left(\frac{n_{pulse}}{4}\right) de_d i_{qs} \qquad (8)$$

Where ids and iqs are the d-and q-hub parts of the stator current of the acceptance motor, individually.

The aggregate DC control at the DC Bridge for all power modules, Pdc, comparing to the real power provided to the enlistment motor can be computed as takes after:

$$P_{dc} = \left(\frac{n_{pulse}}{2}\right) P_{dc\_per\,module} = \left(\frac{n_{pulse}}{2}\right) e_d i_I \quad (9)$$

Where, iI is the DC link current entering the inverter inside each power module. Ignoring losses at the inverters inside power modules, the following equation is satisfied

$$P_{ac\_IM} = P_{dc}. \quad (10)$$

$$\left(\frac{n_{pulse}}{4}\right) de_d i_{qs} = \left(\frac{n_{pulse}}{2}\right) e_d i_I. \quad (11)$$

The DC link current entering the inverter iI , the DC link current after the converter/rectifier id , the DC link voltage before the inverter ed , and the capacitance of the DC link capacitor Cdc have the following relationship

$$i_I = i_d - C_{dc}\frac{de_d}{dt}. \quad (12)$$

$$\frac{1}{2}de_d i_{qs} = e_d\left(i_d - C_{dc}\frac{de_d}{dt}\right). \quad (13)$$

The q-axis component of the motor stator current can be determined from (13) as follows:

$$i_{qs} = \frac{2i_d}{d} - 2C_{dc}\left(\frac{de_d}{dt}\frac{1}{d}\right). \quad (14)$$

Linearize (14), the following can be determined:

$$\Delta i_{qs} = \frac{2}{d_0}\Delta i_d - \frac{i_{qs0}}{d_0}\Delta d - \frac{2C_{dc}}{d_0}S\Delta e_d \quad (15)$$

where S is the Laplace Transform variable.

B. Modelling Of The Control Scheme

The control system utilized as a part of load demonstrating of the medium voltage motor drive system is the shut circle voltage per Hz control. In the event that an alternate control strategy is utilized, conditions for control systems should be balanced in like manner.

Reference [11] gives data on the voltage control technique for the obligation cycle modulator. The objective is to get the suitable obligation cycle(s) and the converter reference outline position so as to accomplish a coveted quick normal synchronous reference outline direct-and quadrature-pivot voltages [11]. The voltage order identified with the obligation cycle adjustment can be communicated as takes after [11]

$$\begin{bmatrix} v_{qs}^e \\ v_{ds}^e \end{bmatrix} = \begin{bmatrix} \cos\theta_{ce} & \sin\theta_{ce} \\ -\sin\theta_{ce} & \cos\theta_{ce} \end{bmatrix}\begin{bmatrix} v_{qs}^c \\ v_{ds}^c \end{bmatrix} \quad (16)$$

Where θ_{ce} is angular displacement of the converter reference frame from the synchronous reference frame, and

$$\theta_{ce} = \theta_c - \theta_e. \quad (17)$$

In this examination work, the sine-triangle PWM is considered. Supplanting V^e_{qs} with the instructed esteem V^{e*}_{qs} , replacing V^e_{ds} with the summoned esteem V^{e*}_{ds} , and replacing V^c_{qs} and V^c_{ds} with the average values expression by (6) and (7) yield

V^{e*}_{ds} , and replacing V^c_{qs} and V^c_{ds} with the average values expression by (6) and (7) yield

$$\begin{bmatrix} v_{qs}^{e*} \\ v_{ds}^{e*} \end{bmatrix} = \begin{bmatrix} \cos\theta_{ce} & \sin\theta_{ce} \\ -\sin\theta_{ce} & \cos\theta_{ce} \end{bmatrix}\begin{bmatrix} v_{qs} \\ v_{ds} \end{bmatrix}$$
$$= \begin{bmatrix} \cos\theta_{ce} & \sin\theta_{ce} \\ -\sin\theta_{ce} & \cos\theta_{ce} \end{bmatrix}\begin{bmatrix} \frac{n_{pulse}}{6}de_d \\ 0 \end{bmatrix}. \quad (18)$$

From (18), the following relationships are obtained.

$$d = \frac{\sqrt{\left(v_{qs}^{e*}\right)^2 + \left(v_{ds}^{e*}\right)^2}}{\left(\frac{n_{pulse}}{6}\right)e_d}. \qquad (19)$$

The block diagram for the closed-loop voltage per Hz control scheme used in this study is shown in Fig. 2. The equations for the closed-loop voltage per Hz control are given as follows.

$$\omega_{SL} = K_{pm}\left(\omega_r^* - \omega_r\right) + \int_0^t K_{im}\left(\omega_r^* - \omega_r\right)dt$$
$$+ \left(\omega_{s0} - \omega_{r0}\right) \qquad (20)$$

$$\omega_{SL} + \omega_r = \omega_s \qquad (21)$$

$$d = \frac{\omega_s \left(\frac{V_b}{\omega_b}\right)\sqrt{2}}{\left(\frac{n_{pulse}}{6}\right)e_d} \qquad (22)$$

$$V_{qs}^{e*} = \omega_s \left(\frac{V_b}{\omega_b}\right)\sqrt{2} \qquad (23)$$

$$V_{ds}^{e*} = 0 \qquad (24)$$

where, Kpm is speed proportional-integral (PI) controller proportional gain; Kim is speed PI controller integral gain;

V_b is the ostensible voltage of the motor per phase; ω_l is the electric precise speed of the rotor in rad/s for the acceptance motor; ω_{sl} is the slip rakish speed of the rotor in rad/s. The parameters with a star as the superscript are reference parameters, and with 0 as the subscript are introductory esteems
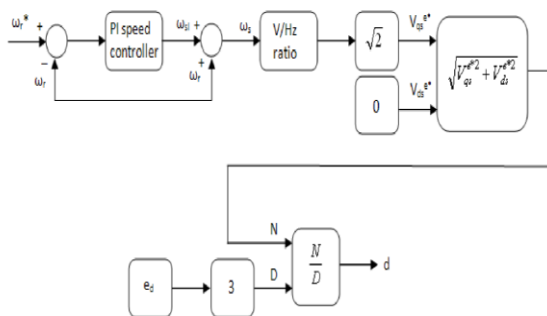
Figure 2. Closed-loop voltage per Hz control scheme for the 18-pulse cascaded H-bridge multi-level inverter motor drive system.

. Liberalize (20) and (21), the bridge amongst ω_s and ω_r can be resolved as takes after.

C. The Derived Dynamic Load Model For The Motor Drive System

At the contribution of the drive, the genuine and receptive power at each power module are the same, and in this manner, the aggregate genuine power (Pac) and responsive power (Qac) can be communicated by the power module number, npulse/2, duplicated by the genuine and receptive power for each power module as takes after (for instance, for a 18-beat drive, the power module number is 9).

$$P_{ac} = \left(\frac{n_{pulse}}{2}\right)P_{ac\_per\,mod\,ule} \qquad (25)$$

$$Q_{ac} = \left(\frac{n_{pulse}}{2}\right)Q_{ac\_per\,mod\,ule} \qquad (26)$$

$$P_{ac\_per\,mod\,ule} = \frac{3}{2}\left(V_{dg}i_{dg} + V_{qg}i_{qg}\right) \qquad (27)$$

$$Q_{ac\_per\,mod\,ule} = \frac{3}{2}\left(-V_{dg}i_{qg} + V_{qg}i_{dg}\right) \qquad (28)$$

$$V_{qg} = \sqrt{2}E \qquad (29)$$

$$V_{dg} = 0 \qquad (30)$$

where, Vdg and Vqg are d-and q-hub control source voltage per phase at the contribution of each power module. By joining differential conditions of the converter, the DC bridge, the inverter, the enlistment motor and the control system, and directing linearization for the entire arrangement of differential conditions of the general system, the identical dynamic model for the medium voltage motor system is acquired as takes after.

$$P = P_0 + G_{P1}\Delta E + G_{P2}\Delta E^2 + (G_{P3} + G_{P4}\Delta E)\Delta f_g \quad (31)$$
$$Q = Q_0 + G_{Q1}\Delta E + G_{Q2}\Delta E^2 + (G_{Q3} + G_{Q4}\Delta E)\Delta f_g. \quad (32)$$

(a)

(b)
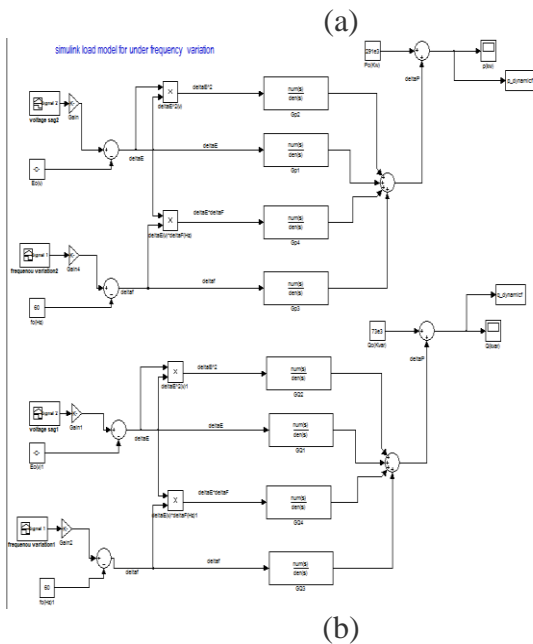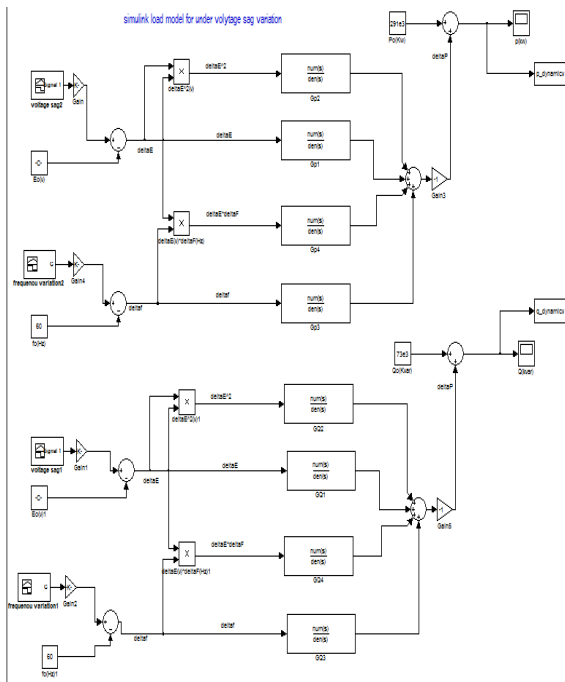
Figure 3. Simulink model and its schematic diagram based on the developed model for the sample system: (a) Simulink model voltage sag variations (b) Simulink model for frequency variations

The coefficients (GPi, GQi, i D 1, 2, 3, 4) in (31)-(32) are the 7th order transfer functions. The proposed dynamic model is expressed by these coefficients. Both voltage and frequency

$$G_{Pi} = \frac{\left(GP_{i1}S^7 + GP_{i2}S^6 + GP_{i3}S^5 + GP_{i4}S^4 + \atop GP_{i5}S^3 + GP_{i6}S^2 + GP_{i7}S + G_{i8} \right)}{\left(P_{b1}S^7 + P_{b2}S^6 + P_{b3}S^5 + P_{b4}S^4 + \atop P_{b5}S^3 + P_{b6}S^2 + P_{b7}S + P_{b8} \right)}$$
$$(i = 1, 2, 3, 4) \quad (33)$$

$$G_{Qi} = \frac{\left(GQ_{i1}S^7 + GQ_{i2}S^6 + GQ_{i3}S^5 + GQ_{i4}S^4 + \atop GQ_{i5}S^3 + GQ_{i6}S^2 + GQ_{i7}S + GQ_{i8} \right)}{\left(P_{b1}S^7 + P_{b2}S^6 + P_{b3}S^5 + P_{b4}S^4 + \atop P_{b5}S^3 + P_{b6}S^2 + P_{b7}S + P_{b8} \right)}$$
$$(i = 1, 2, 3, 4) \quad (34)$$

$$\Delta E = E - E_0 \quad (35)$$

$$\Delta f_g = f_g - f_{g0} \quad (36)$$
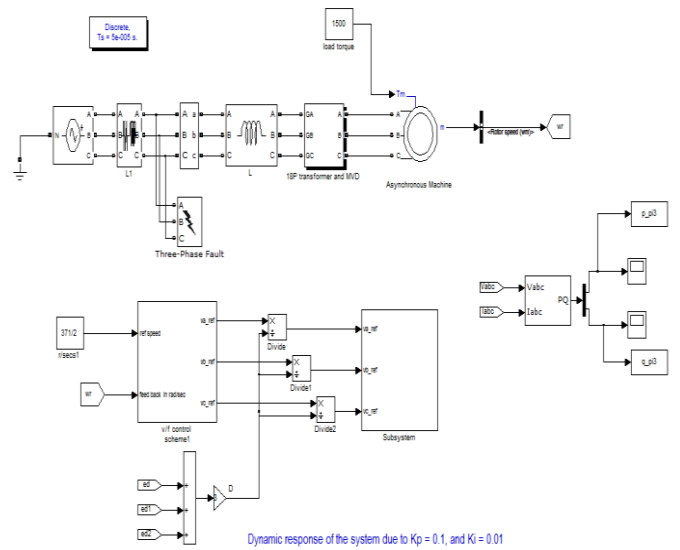
Figure 4. Detailed switching model for the sample system built using Simulink.

The sample system consists of an 18-pulse medium voltage cascaded H-bridge multi-level voltage source inverter drive, and an induction motor rated at 2300 V and 1500 HP. The control scheme is the closed-loop voltage per Hz control.

Simulations:

Case1:

Three-phase fault is connected to the drive input, which causes a 90% voltage hang in the nitty gritty exchanging model. The fault begins from 14.4 s also, is cleared at 14.65 s, and the recurrence of the power source continues as before. The aggregate recreation time utilizing Matlab/Simulink is 15 seconds.

(a)

(b)

(c)
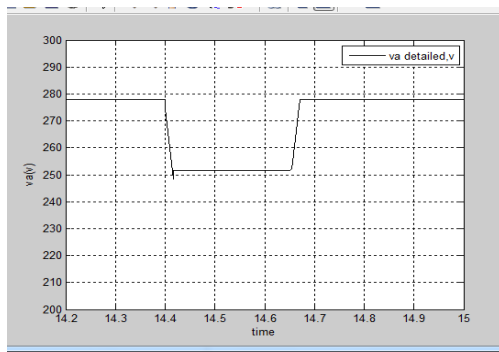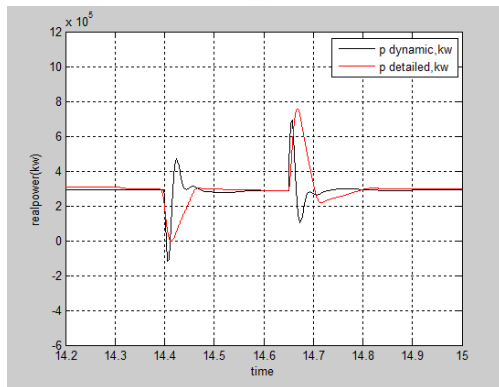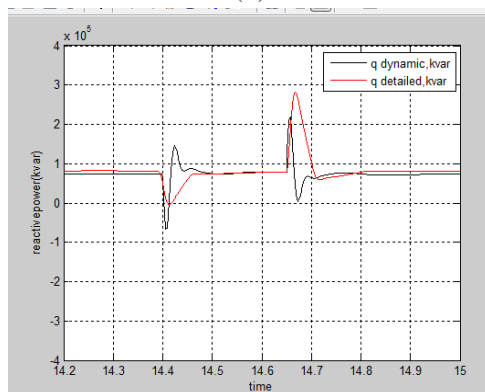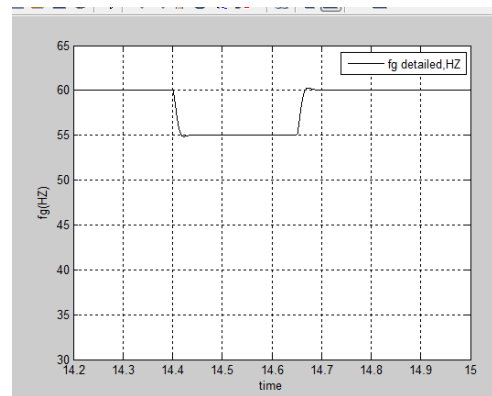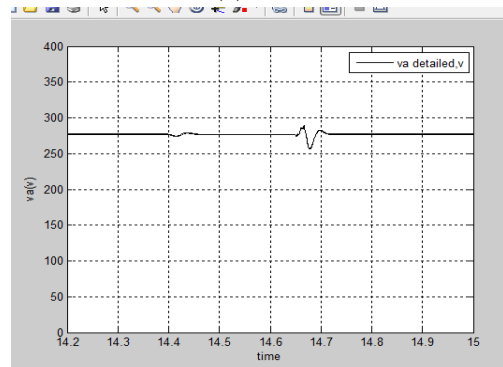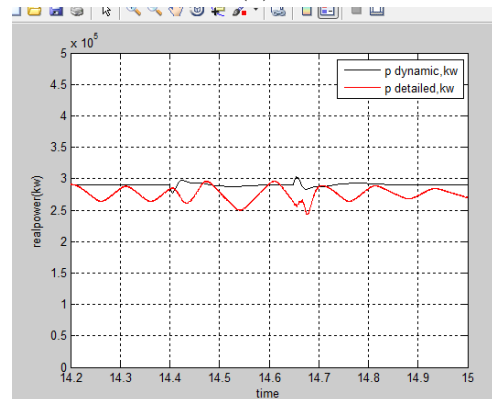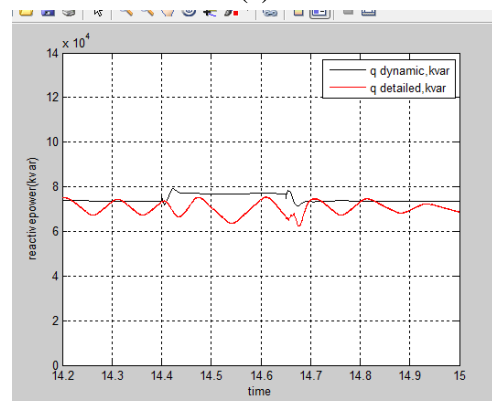
Figure 5. Dynamic response of the developed dynamic load model and the detailed switching model of the sample system when subjected to a 90% voltage sag: (a) voltage sag, (b) real power P, and (c) reactive power Q.

Case2:

To verify the frequency dependence characteristic of the proposed dynamic load model, a frequency variation step changed from 60 Hz to 55 Hz is applied at the power source in the detailed switching model. This frequency variation starts from 14.4 s and is cleared at 14.65 s. The total simulation time using Matlab/Simulink is 15 seconds

(a)

(b)

(c)

(d)

Figure 6. Dynamic response of the developed dynamic load model and the detailed switching model for a frequency variation: (a) frequency variation, (b) voltage variation, (c) real power P, and (d) reactive power Q.

Case3:

this type of motor drive systems, and is suitable for power systems dynamic studies considered: (1) Kp = 1:25, and Ki = 1:6; (2) Kp = 9, and Ki = 10; (3) Kp = 0:1, and Ki = 0:01.
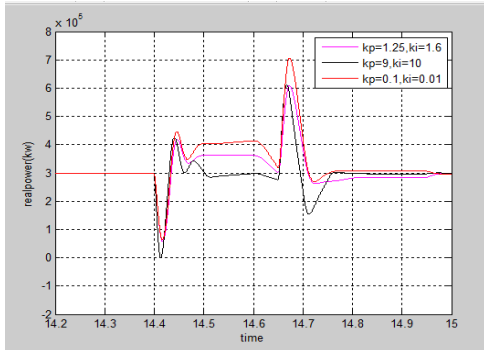
(a)
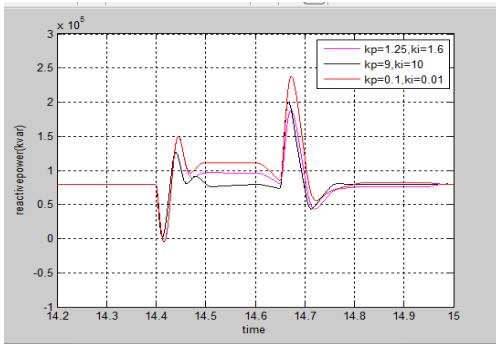

(b)

Figure 7. Dynamic response of the developed dynamic load model due to different speed controller parameters, Kp and Ki: (a) real power P and (b) reactive power Q.

Case4:

Dynamic response of the developed dynamic model due to different DC link capacitance Cdc of each power module inside the medium voltage drive. The Cdc values are 9200 uF, 10000uF and 18000 uF. Other parameters
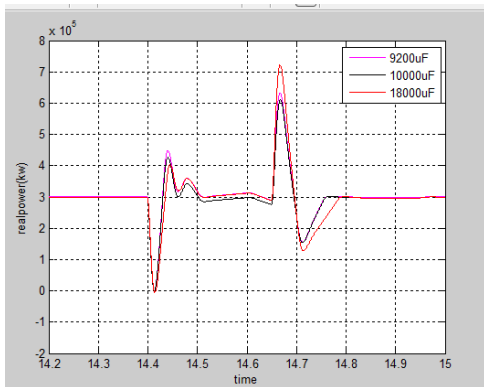
(a)
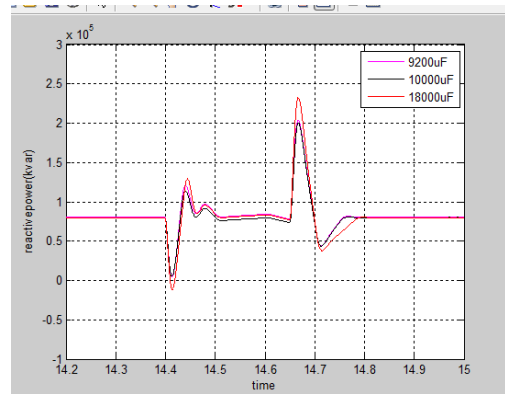
(b)

Figure 8. Dynamic response of the developed dynamic model due to different DC link capacitance Cdc of each power module inside the medium voltage drive: (a) real power P and (b) reactive power Q.

case5:

Three different load torques TL are applied to the induction motor for the proposed dynamic model when subjected to a 90% voltage sag: 1000 Nm, 1500 Nm and 2000 Nm
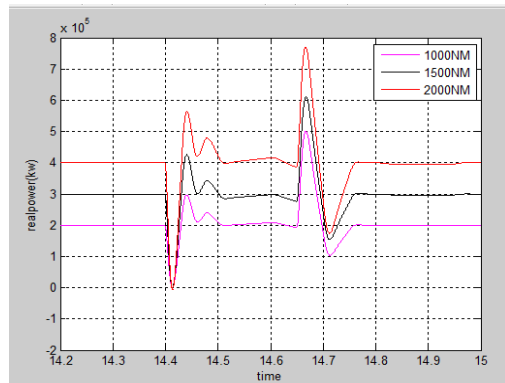
(a)
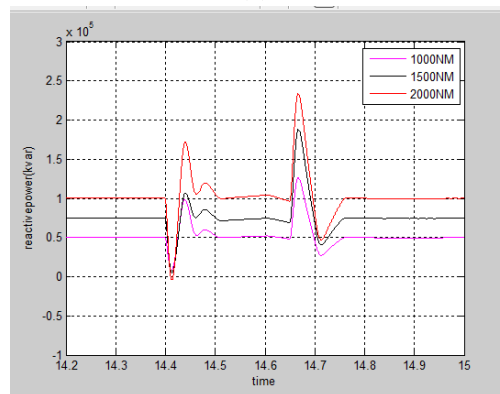
(b)

Figure 9. Dynamic response of the developed dynamic model due to different load torque of the induction motor TL: (a) real power P and (b) reactive power Q.

Fuzzy logic

Fuzzy technique for thinking is a kind of different respected avocation in which reality estimations of factors might be any true blue number some place around 0 and 1. By partition, in Boolean strategy for thinking, reality estimations of factors may just be 0 or 1. Fuzzy technique for thinking has been reached out to handle the likelihood of halfway truth, where reality quality may extend between completely certifiable and totally false. Moreover, when etymological factors are utilized, these degrees might be managed by particular points of confinement.

Routinely Fuzzy technique for thinking control structure is delivered utilizing four immense sections showed on Figure fuzzification interface, Fuzzy insincerity motor, cushy standard system and Defuzzification interface. Every part near to foremost Fuzzy strategy for thinking operations will be depicted in more detail below.

The Fuzzy technique for thinking examination and control approaches appeared in Figure 1 can be depicted as:

1. Receiving one or sweeping number of estimations or other assessment of conditions existing in some system that will be investigated or controlled.
2. Processing all got contributions as appeared by human based, Fuzzy "expecting then" models, which can be granted in fundamental dialect words, and joined with normal non-Fuzzy arranging.
3. Averaging and weighting the outcomes from all the individual norms into one single yield choice or sign which picks what to do or urges a controlled system what to do. The outcome yield sign is an exact defuzzified respect. Most importantly else, the unmistakable level of yield (fast, low speed etc...) of the stage is described by deciding the cooperation capacities with respect to the fuzzy sets.

Fuzzy Logic System

Today control systems are normally portrayed by numerical models that take after the laws of material science, stochastic models or models which have risen up out of scientific rationale. A general trouble of such built model is the manner by which to move from an offered issue to an appropriate numerical model. Without a doubt, today's propelled PC innovation makes it conceivable; however overseeing such systems is still excessively perplexing. These perplexing systems can be rearranged by utilizing a resilience edge for a sensible measure of imprecision, dubiousness and instability amid the demonstrating stage. As a result, not totally consummate system comes to presence; by and by in the greater part of the cases it is equipped for taking care of the issue in proper way. Notwithstanding missing information data has officially ended up being agreeable in learning based systems.

## Simulation model using fuzzy logic controller:
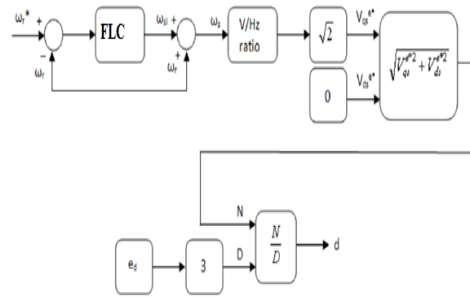
Figure 10. Closed-loop voltage per Hz control scheme for the 18-pulse cascaded H-bridge multi-level inverter motor drive system using fuzzy logic controller.

Case1:
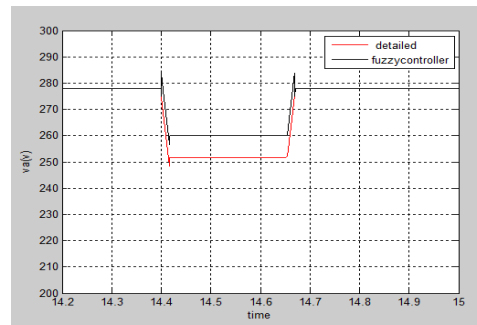

(a)
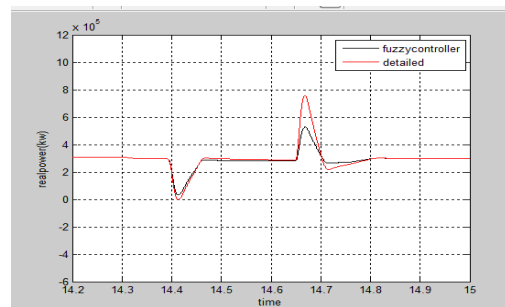
(b)
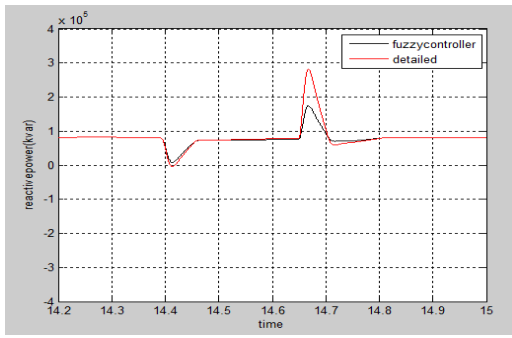
(c)

Figure 11. Dynamic response of the developed dynamic load model and the detailed switching model of the sample system when subjected to a 90% voltage sag using fuzzy logic controller: (a) voltage sag, (b) real power P, and (c) reactive power Q.

case2:

(a)

(b)

(c)
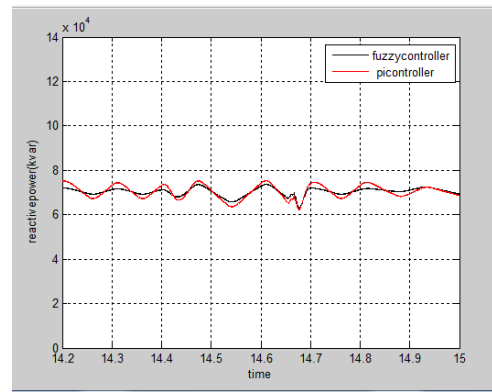
(d)

Figure 12. Dynamic response of the developed dynamic load model and the detailed switching model for a frequency variation using fuzzy logic controller: (a) frequency variation, (b) voltage variation, (c) real power P, and (d) reactive power Q.
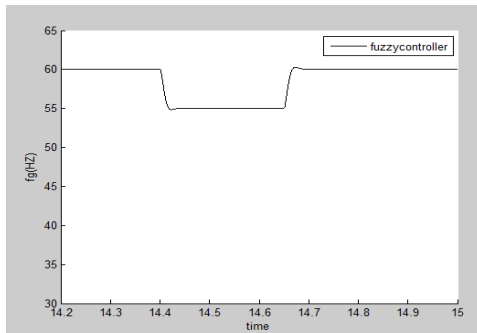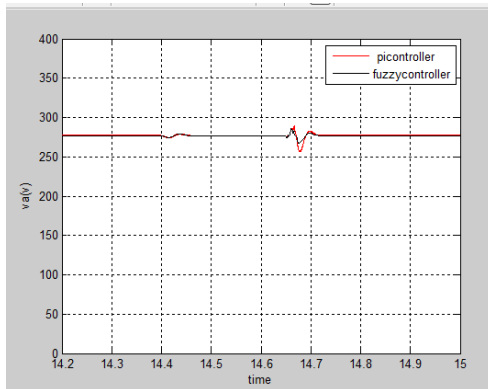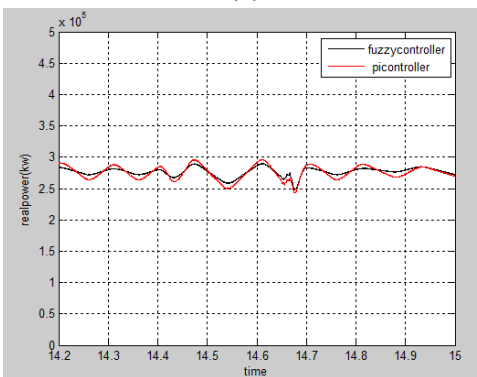
Case3:
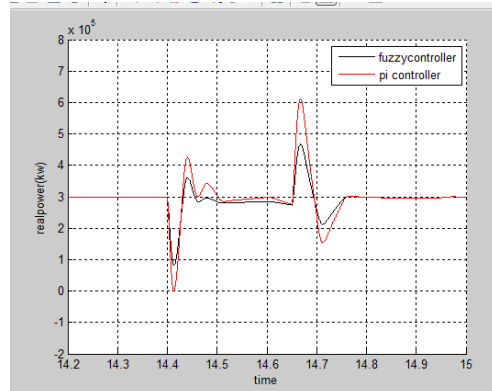
(a)
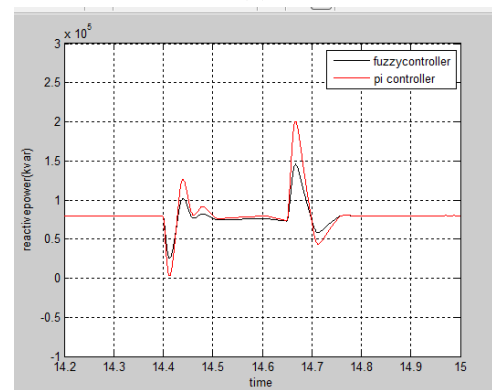
(b)

Figure 13. Dynamic response of the developed dynamic load model due to different speed controller parameters using fuzzy logic controller, Kp and Ki:(a) real power P and (b) reactive power Q.

Case4:
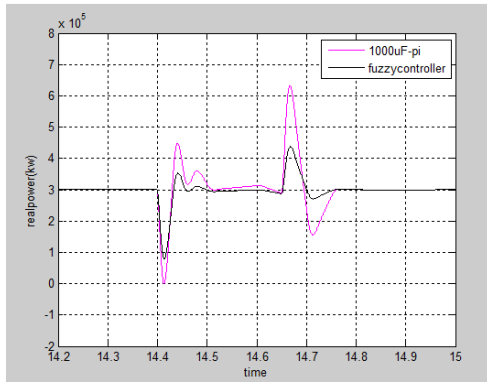
(a)
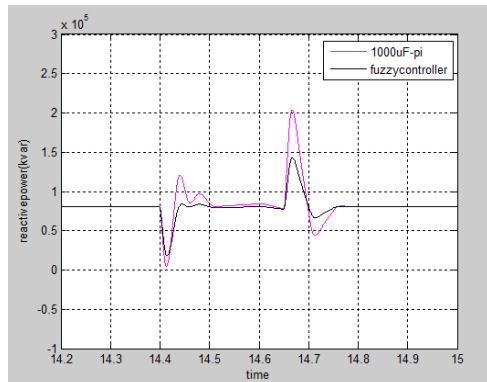
(b)

Figure 14. Dynamic response of the developed dynamic model due to different DC link capacitance Cdc of each power module inside the medium voltage drive using fuzzy logic controller: (a) real power P and (b) reactive power Q.

case5:
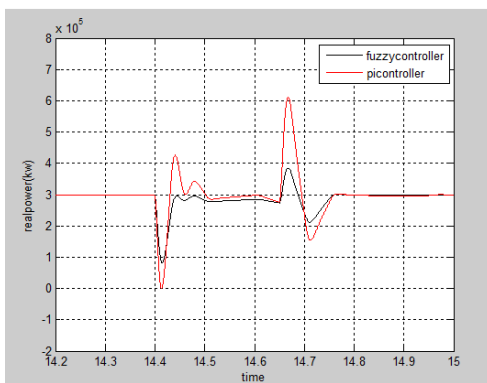
(a)
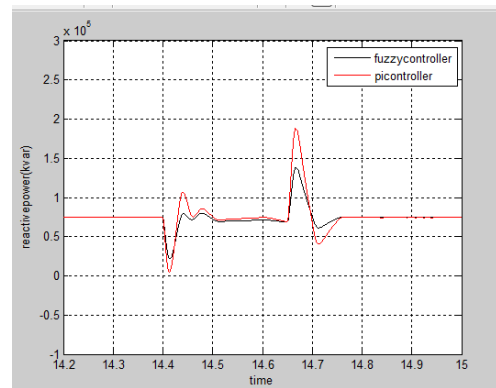
(b)

Figure 15. Dynamic response of the developed dynamic model due to different load torque of the induction motor using fuzzy logic controller TL: (a) real power P and (b) reactive power Q.

III. CONCLUSION

The dynamic load display for a medium voltage cascaded H-bridge multi-level PWM inverter motor drive system is created in this paper, which is inferred utilizing a scientific strategy called the linearization approach. The exactness of the proposed demonstrate is verified by a contextual analysis utilizing a specimen medium voltage motor drive system. The influence of key parameters of the model on unique reaction qualities is assessed through an affectability think about. The created dynamic load model of the medium voltage motor drive system is communicated by seventh request exchange

capacities with both voltage and recurrence reliance considered. Compare the medium voltage cascaded H-bridge multi level inverter drive and induction motor system using fuzzy logic controller with pi controller. Fuzzy logic controller gives the better performance compared to pi controller.

IV. REFERENCES

[1]. IEEE Task Force on Load Representation for Dynamic Performance, 'Load representation for dynamic performance analysis [of power systems],'IEEE Trans. Power Syst., vol. 8, no. 2, pp. 472_482, May 1993.

[2]. IEEE Task Force on Load Representation for Dynamic Performance, 'Standard load models for

power and dynamic performance simulation,'IEEE Trans. Power Syst., vol. 10, no. 3, pp. 1302_1313, Aug. 1995.

[3]. A. Merdassi, L. Gerbaud, and S. Bacha, 'A new automatic average modelling tool for power electronics systems,'in Proc. IEEE Power Electron.Specialists Conf. (PESC), Jun. 2008, pp. 3425_3431.

[4]. J. Sun and H. Grotstollen, 'Averaged modelling of switching power converters: Reformulation and theoretical basis,'in Proc. IEEE 23rd Annu. Power Electron. Specialists Conf. (PESC), vol. 2. Jun./Jul. 1992, pp. 1165_1172.

[5]. S. Cuk and R. D. Middlebrook, 'A general uni_ed approach to modeling switching-converter power stages,'in Proc. IEEE Annu. Power Electron. Specialists Conf. (PESC), Jun. 1976, pp. 18_31.

[6]. A. Griffo, J. B. Wang, and D. Howe, 'State-space average modelling of 18-pulse diode recti_er,'in Proc. 3rd Int. Conf. Sci. Comput. Comput. Eng. (IC-SCCE), Jul. 2008, pp. 1_8.

[7]. T. A. Meynard, M. Fadel, and N. Aouda, 'Modeling of multilevel converters,'IEEE Trans. Ind. Electron., vol. 44, no. 3, pp. 356_364, Jun. 1997.

[8]. A. Uan-Zo-li, R. P. Burgos, F. Lacaux, F. Wang, and D. Boroyevich, 'Assessment of multipulse converter average models for stability studies using a quasistationary small-signal technique,'in Proc. 4th Int. Power Electron. Motor Control Conf., vol. 3. Aug. 2004, pp. 1654_1658.

[9]. S. Rosado, R. Burgos, F. Wang, and D. Boroyevich, 'Large- and small signal evaluation of average models for multi-pulse diode recti_ers,'in Proc. IEEE Workshops Comput. Power Electron. (COMPEL), Jul. 2006,pp. 89_94.

[10]. A. Emadi, A. Khaligh, C. H. Rivetta, and G. A. Williamson, 'Constant power loads and negative impedance instability in automotive systems: De_nition, modeling, stability, and conrol of power electronic converters and motor drives,'IEEE Trans. Veh. Technol., vol. 55, no. 4, pp. 1112_1125, Jul. 2006.

[11]. P. C. Krause, O. Wasynczuk, and S. D. Sudhoff, Analysis of Electric Machinery and Drive Systems, 2nd ed. Piscataway, NJ, USA: IEEE Press, 2002.

[12]. S. A. Y. Sabir and D. C. Lee, 'Dynamic load models derived from date acquired during system transients,'IEEE Trans. Power App. Syst.,

[13]. vol. PAS-101, no. 9, pp. 3365_3372, Sep. 1982.

[14]. T. Omata and K. Uemura, 'Effects of series impedance on power system load dynamics,'IEEE Trans. Power Syst., vol. 14, no. 3, pp. 1070_1077, Aug. 1999.

[15]. F. T. Dai, J. V. Milanovic, N. Jenkins, and V. Roberts, 'Development of a dynamic power system load model,'in Proc. 7th Int. Conf. AC-DC Power Transmiss., Nov. 2001, pp. 344_349.

[16]. X. Liang and W. Xu, 'Modeling variable frequency drive and motor systems in power systems dynamic studies,'in Proc. IEEE Ind. Appl. Soc. (IAS) Annu. Meeting, Oct. 2013, pp. 1_11.